13th World Conference on Earthquake Engineering
Vancouver, B.C., Canada
August 1-6, 2004
Paper No. 1029

AN INVESTIGATION OF THE EARTHQUAKE EFFECTS ON ARTICULATED BRIDGES LOCATED ON FAULT RUPTURES

Turel GUR[1] and Mete A. SOZEN[2]

SUMMARY

The bridges on the surface rupture of the 1999 earthquakes in Taiwan and Turkey were severely affected by permanent deformations of the ground. The post-earthquake states of these structures are described briefly. The earthquake effects on the 2.3-km Bolu Viaduct in Turkey crossed by the surface rupture of the 1999 Duzce earthquake are investigated in detail. A simple inelastic model of the bridge is analyzed by using the acceleration records of the Marmara and Duzce earthquakes. The calculated response does not provide an explanation for the observed damage. The results of these analyses indicate that the response of the Bolu Viaduct is sensitive the PGV of the records rather than their PGA's. In addition, the response of the viaduct to ground distortion is evaluated by introducing pier movements as an input assuming that they occurred in a few seconds. The results of the analyses suggest that the severe damage to the viaduct was caused by the rapid distortion of the ground.

INTRODUCTION

Long articulated bridges may sustain earthquake damage not only by the shaking but also by the distortion of the ground if the rupture zone is within the footprint of the structure. Recent examples of such events were provided by the 1999 earthquakes in Taiwan (921 Chi-Chi) and in Turkey (Marmara and Duzce) [1, 2, 3]. Some of these are described briefly in Fig. 1. The post-earthquake observations at these bridge sites reveal the fact that the ground deformations created a permanent relative movement of the supports with respect to each other which is not an effect routinely considered in the design. The type of the fault rupture determines the direction of the relative movement of the supports. The thrust fault rupture observed at the bridge sites in Taiwan created elevation difference between the supports leading to the collapse of the girders. The piers of these bridges were observed to be tilted during the vertical movement of the ground. On the other hand, the strike-slip type of fault rupture between the piers of the Arifiye Overpass in Turkey during the Marmara earthquake moved the supports away from each other so that the girders of the northernmost span could not be supported anymore.

[1] Research Assistant, Dept. of Civil Eng., Purdue University, West Lafayette, IN 47907
[2] Kettelhut Distinguished Professor of Civil Eng., Dept. of Civil Eng., Purdue University, West Lafayette, IN 47907

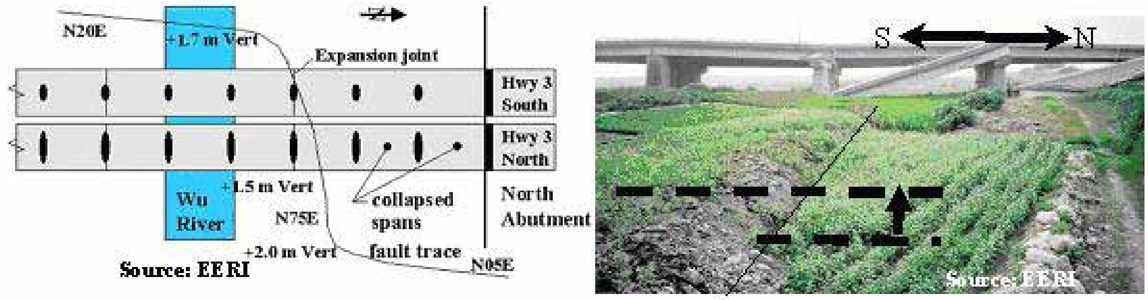

Plan view Elevation view

Wu-Shi Bridge, Taiwan (Southern portion rose 1.5-2 m with respect to the northern abutment.)

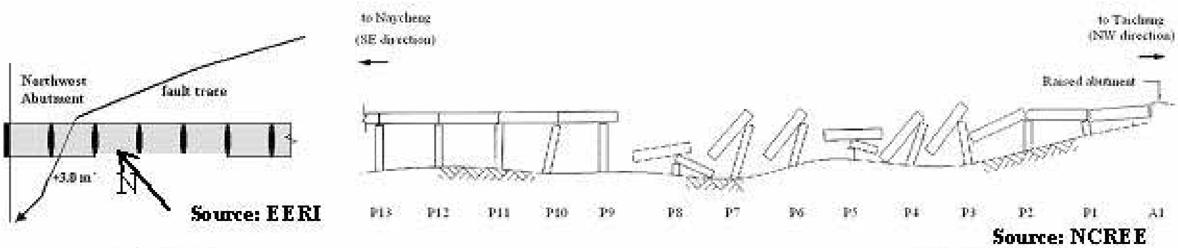

Plan view Elevation view

Yi-Jiang Bridge, Taiwan (Northern abutment elevated 3 m compared to the rest of the bridge. The bridge was compressed 4 m in the longitudinal direction)

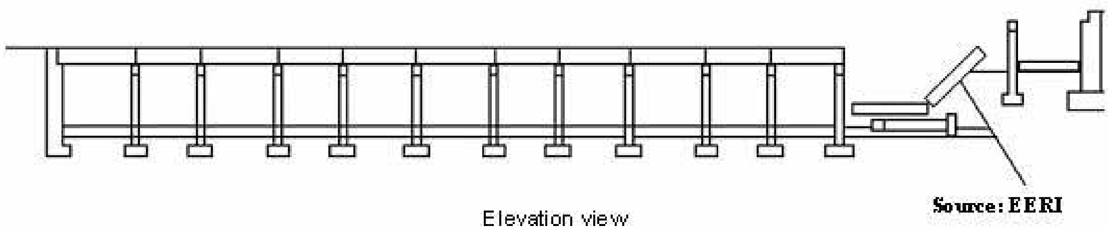

Elevation view

Bei-Feng Bridge, Taiwan (The vertical movement at the fault was 3 m.)

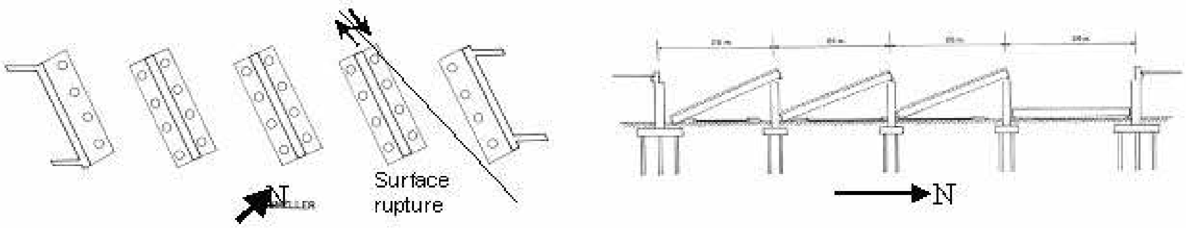

Plan view Elevation view

Arifiye Overpass, Turkey (The first span at the north end became wider than the girders.)

Figure 1. The bridges in Taiwan and Turkey which collapsed during the 1999 earthquakes

In addition to the other examples of the bridges on fault ruptures mentioned above, the Bolu Viaduct in Turkey (Fig.2) was crossed by the surface rupture of the 1999 Duzce earthquake. The viaduct, which was not yet open to the traffic, was affected by the Marmara earthquake, as well. The positions of the girders and the piers were surveyed in detail before and after the earthquakes. The 2.3-km viaduct comprises two parallel carriageways. The piers, located at every 39.2 m, are supported by 20-30 m deep pile groups composed of 12 reinforced concrete drilled piles (Fig. 3a and 3b). Except at the ends of the viaduct, the piers range in height from 44 to 49 m. The piers have cast-in-place hollow sections (Fig. 3c). There are seven precast and pretensioned girders in each span of each carriageway. The girders rest on free sliding bearings. The slab was cast continuously with an expansion joint every tenth span. The deck is connected to each pier through energy-dissipating units (EDU) that permit a maximum relative movement of 0.48 m between the deck and the pier (Fig. 3d).

Figure 2. The Bolu Viaduct

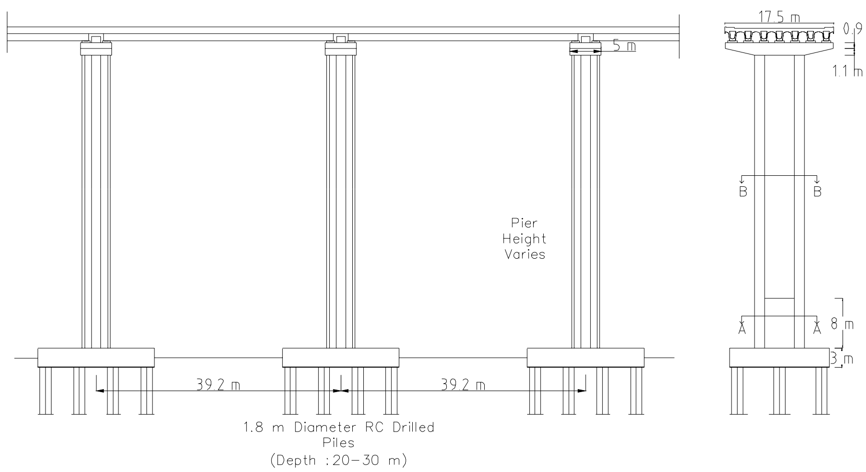

(a) **(b)**

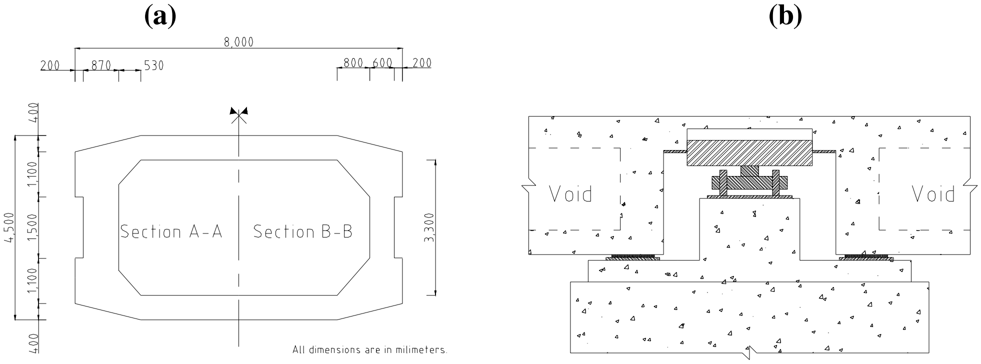

(c) **(d)**

Figure 3. Dimensions and details of the Bolu Viaduct. a) Side view, b) Transverse direction c) Pier cross sections, d) Side view of the joint between the deck and piers

THE 1999 EARTHQUAKES IN TURKEY AND THEIR EFFECTS OF ON THE VIADUCT

17 August 1999 Marmara Earthquake (Mw=7.4)

The Marmara earthquake struck northwestern Turkey on August 17, 1999 at 3:02 am local time. The surface rupture of the earthquake was estimated to be 140 km. The only acceleration record of the earthquake in the vicinity of the viaduct was at Duzce, which is 17 km away from the viaduct site. The other closest station at Bolu, 22 km away from the viaduct, was not triggered by the ground shaking.

The viaduct site was approximately 30 km away from the east end of the surface rupture. The earthquake was felt strongly at the viaduct site. Although there was no structural damage, some prefabricated beams in stock and some equipment at the site were damaged [4]. The energy dissipating devices were reported to have performed satisfactorily. Inspection teams measured the tracks of the displacements left by the girder bearings on the stainless steel sliding plates. The maximum shift of the girders with respect to the piers was measured to be 90 mm. This implies that the energy dissipating devices were forced beyond their yield level. It was also reported that the girders returned back to their initial positions without leaving "significant residual displacement".

12 November 1999 Duzce Earthquake (Mw=7.1)

The Bolu-Duzce region was struck by another strong earthquake on November 12, 1999 at 7:57 pm local time. The surface rupture started from the eastern end of the surface rupture of the event on August 17 and extended east approximately 45 km. The epicenter of the event was estimated to be at 7 km south of Duzce.

The permanent strong motion stations at Duzce (DZC) and Bolu (BOL) recorded the motion. In addition, there were other records obtained by 12 temporary stations near Karadere installed for the aftershocks at the end region of the Marmara earthquake fault. Six of the stations (stations DZC, BOL, 375, 487, 496 and 498) recorded horizontal accelerations exceeding 30% of the gravitational acceleration and the approximate locations of these stations are shown in Fig. 4. The highest horizontal acceleration of 10 m/s2 was recorded at station 496.

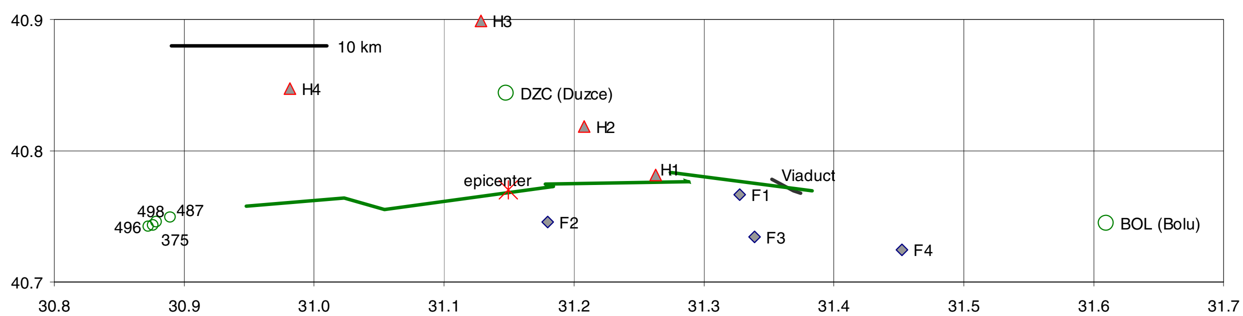

Figure 4. The surface rupture of the Duzce earthquake. Triangles and diamonds indicate the locations of the GPS stations. Circles show the location of the strong motion stations.

There are two types of ground deformation measurements available in the Duzce fault rupture region. Akyuz et al. [5] mapped the surface trace and indicated the amount of slip along the trace whereas Burgmann et al. [6] monitored the absolute ground displacements at the GPS stations established in the region prior to the 1999 events. The locations of the GPS stations are marked on Fig. 4. The absolute displacements measured at the GPS stations conforms the right-lateral strike-slip characteristics of the fault rupture. The GPS data and the surface slip measurements can be compared as follows:

- Stations H1 and H2 drifted 2.8 and 1.7 m toward east, respectively. The slip at the fault in this region was observed to be between 3.1 and 4.2 m. Station H1 is very close to the surface trace whereas station H2 is located 4 km away. It can be inferred that most of the right-lateral movement occurred in the northern plate in this region (Fig. 5). It is also interesting to note that the displacement measured 4 km away from the surface trace is approximately half the displacement observed right at the trace.
- The westward movement at Station F1 was 1.1 m (Fig. 5). The slip observed near station F1 was in the range of 2.4 to 3.0 m. The contribution of the movement of the southern plate to the overall slip

should be less than that of the northern plate. It can be concluded that the ratio of the movement of the northern plate to that of the southern plate is approximately 2.

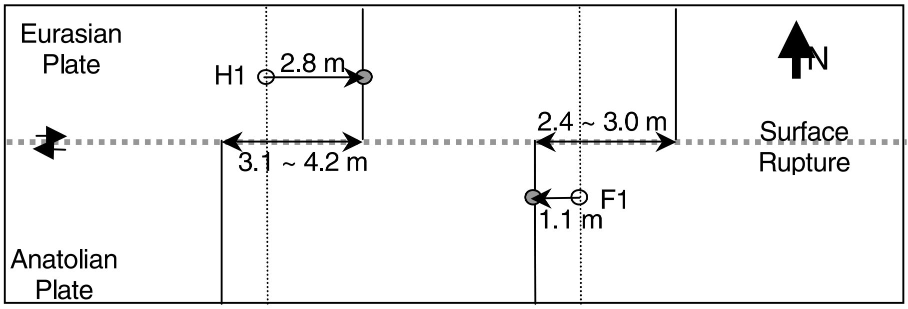

Figure 5. Comparison of the absolute displacements of the GPS stations H1 and F1 and the slip observed at the surface rupture. Thin vertical lines are imaginary lines perpendicular to the surface rupture before the slip. The hollow and full circles indicate the locations of the stations before and after the earthquake, respectively.

The Bolu Viaduct lies on the eastern end of the fault segment ruptured during the November 1999 event. The surface trace passed through the bridge at a 15-degree angle with the axis of the bridge. The fault slip under the bridge was measured approximately as 1.5m. The piers of the viaduct experienced permanent displacement. Because of the low angle between the viaduct and the rupture trace, the pier movements were almost parallel to the axis of the viaduct. As a result, the viaduct was shortened by 2.1 m. The shortening was concentrated at the spans next to the rupture. The foundations of the piers on the rupture trace suffered severe damage because of the 2 to 3 degree twist around their own axes. The girders displaced in both longitudinal and transverse directions. The relative movement of the girders with respect to the piers resulted in the failure of the EDU's and the ejection of the bearings under the girders. The girders impacted and destroyed the plinths, concrete blocks supporting the EDU's (Fig. 6).

Figure 6. The damage caused by the relative movements of the girders with respect to the piers

There were two types of measurements of the viaduct available: (1) the GPS measurements of the piers before and after earthquake and (2) the movement of individual girder. The former was used to calculate the change in the relative positions of the piers with respect to each other and the tilting of the piers. It was not possible to calculate the absolute movement of each individual pier because the coordinate systems of the two sets of GPS measurements were different. Based on the observations related with the movement of the plates explained above, it was assumed that the total shortening of 2.1 m was due to a 1.4 m eastward movement at the west abutment and a 0.7 m westward movement at the east abutment. The absolute movement of each individual pier based on this assumption is shown in Fig.7. Another set of data calculated from the measurements of the deformed state of the viaduct is the relative movements of the girders with respect to the pier bases shown in Fig.8. As seen in the figure, the direction of the relative movement of the deck segments is consistently toward west except the eastern and of segment 5.

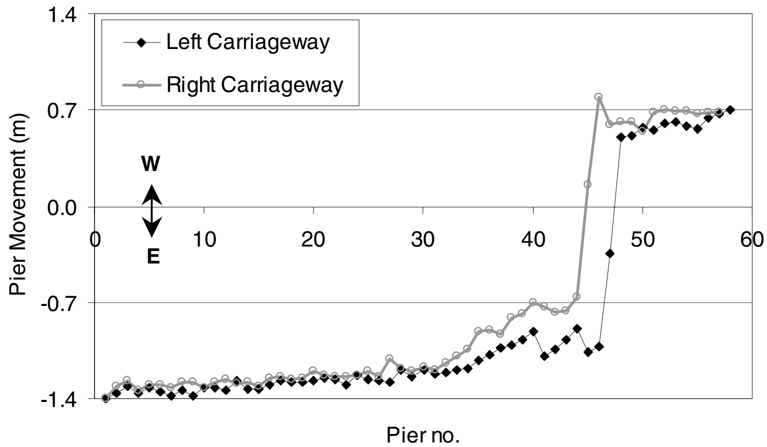

Figure 7. The measured movement of the piers in the longitudinal direction

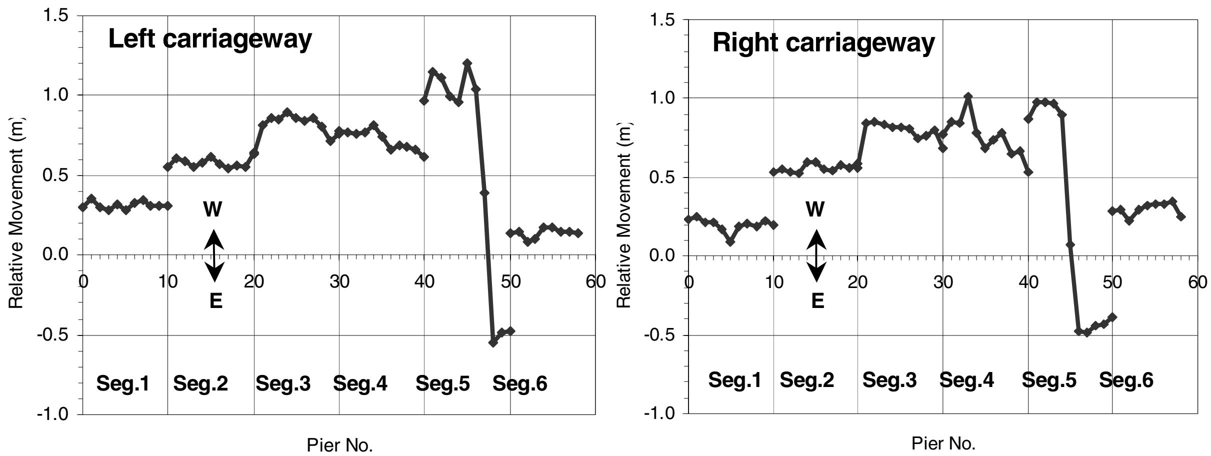

Figure 8. The relative movement of the girders with respect to the pier bases (ground)

INELASTIC RESPONSE OF THE VIADUCT TO GROUND SHAKING

Structural Data for the Analyses

The simplified model of the viaduct (Fig. 9) comprised two nonlinear springs in series. One represented the pier with its mass distributed along its height. The other represented the EDU seated on the pier. The moment of inertia of the pier is 102 m^4 in the transverse direction and 37 m^4 in the longitudinal direction. The mass of the deck was attached to the spring representing the EDU. Another mass representing the mass of the pier cap was lumped at the end of the pier. The masses of the deck, the pier and the pier cap in the model were estimated to be 1540, 1830 and 160 tons, respectively. The elasticity modulus of concrete was taken to be 28 000 MPa. The equations of motion were derived by assuming a shape function for the bending of the pier and solved by using a step-by-step iterative procedure [7]. The critical damping ratio is equal to 0.02 in the analyses.

The function of the EDU's during an earthquake is not only to limit the force transfer between the deck and the piers but also to dissipate the input energy by means of the hysteretic damping. Therefore, inelastic force-deformation characteristics of the elements of the model were used in the response calculation. The force-deformation function defined by Ramberg and Osgood [8] was used in this study. Figure 10 shows the "actual" and the fitted force-displacement relationships of the members in comparison. The actual force-displacement curve of EDU was based on its mechanical properties reported by Marioni [4] whereas the force-displacement curve of the pier was based on the moment-curvature relationship at its bottom section. The reinforcement layout and the material strength provided in the design drawings were used in the calculations. The longitudinal reinforcement ratio at the base of the pier was 2.4%. The steel type was indicated as St50 on the drawings. The design strength of concrete is specified to be 35 MPa. After moment-curvature diagram is obtained, the coordinates of each point on the curve is transformed into force and displacement values by assuming a plastic-hinge length equal to the depth of the section.

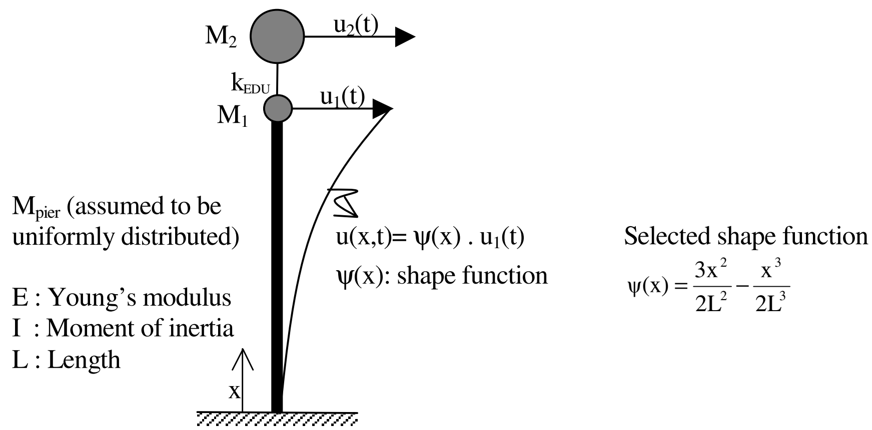

Figure 9. Simplified model of the viaduct for ground shaking

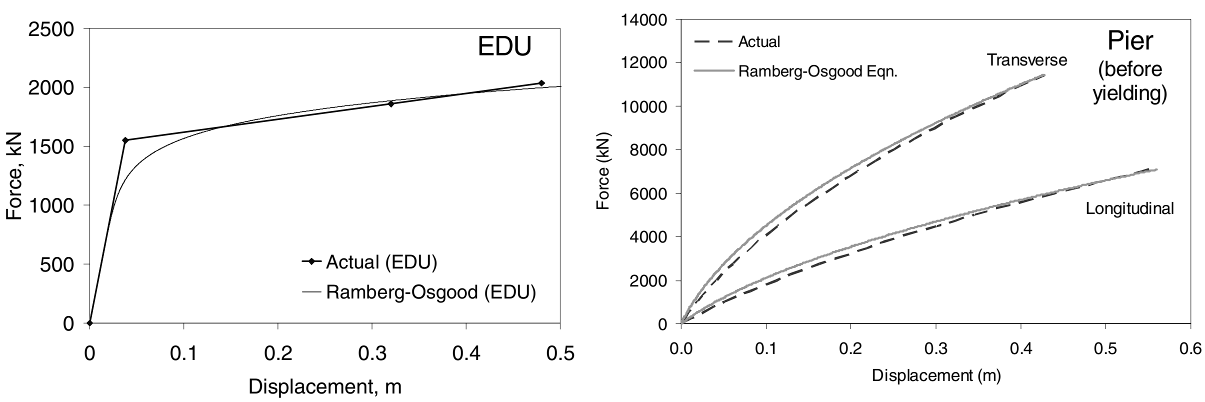

Figure 10. The force-displacement characteristics of the members

Discussion of the Results

The model of the viaduct was analyzed for its inelastic response to the records of the 1999 earthquakes in Turkey. The records of the Marmara and the Duzce earthquakes exceeding 0.3g were used in the analyses. The response of the viaduct in the transverse and the longitudinal directions were calculated independently. The amount of maximum displacement response of the elements of the model, the pier and the EDU, in each analysis is listed with the maxima of the input ground motion in Table 1.

The analyses of the simplified model of the viaduct with the Duzce record of the Marmara earthquake show that the calculated response is much larger than the response observed after the August 1999 event. If the ground motions at Duzce and the site of the viaduct were identical, then the deck of the viaduct would have displaced approximately 0.35 m with respect to the piers in both orthogonal directions. The observed maximum shift of the deck of the bridge with respect to the piers was 0.09 m. The difference between the observed and the calculated maximum response can be attributed to the difference in the soil conditions in Duzce and the viaduct site.

Table 1 The ground motion records used in the dynamic analysis and maximum displacement response of the elements

Record Name	PGA (m/s^2)	PGV (m/s)	Maximum Element Response (m)			
			Transverse Dir.		Longitudinal Dir.	
			Pier	EDU	Pier	EDU
Marmara EQ - Arcelik EW	1.31	0.44	0.03	0.05	0.06	0.04
Marmara EQ - Arcelik NS	2.07	0.17	0.02	0.03	0.04	0.03
Marmara EQ - Duzce EW	3.76	0.57	0.08	0.28	0.13	0.28
Marmara EQ - Duzce NS	3.31	0.57	0.06	0.21	0.15	0.29
Marmara EQ - Gebze EW	1.41	0.34	0.03	0.07	0.07	0.04
Marmara EQ - Gebze NS	2.64	0.47	0.06	0.13	0.09	0.10
Marmara EQ - Izmit EW	2.23	0.52	0.06	0.17	0.15	0.20
Marmara EQ - Izmit NS	1.64	0.31	0.04	0.10	0.08	0.07
Marmara EQ - Sakarya EW	3.99	0.80	0.06	0.18	0.13	0.18
Marmara EQ - Yarimca EW	2.26	0.85	0.08	0.19	0.13	0.23
Marmara EQ - Yarimca NS	3.16	0.75	0.10	0.34	0.16	0.33
Duzce EQ - Bolu EW	8.06	0.67	0.09	0.21	0.12	0.25
Duzce EQ - Bolu NS	7.39	0.58	0.07	0.21	0.12	0.18
Duzce EQ - Duzce EW	5.03	0.84	0.08	0.32	0.18	0.38
Duzce EQ - Duzce NS	4.02	0.65	0.13	0.29	0.13	0.25
Duzce EQ - Karadere 375 EW	4.52	0.18	0.03	0.05	0.03	0.03
Duzce EQ - Karadere 375 NS	8.18	0.37	0.07	0.06	0.05	0.04
Duzce EQ - Karadere 487 EW	2.77	0.29	0.05	0.06	0.04	0.04
Duzce EQ - Karadere 487 NS	2.98	0.39	0.04	0.06	0.06	0.06
Duzce EQ - Karadere 496 EW	7.35	0.40	0.06	0.12	0.06	0.05
Duzce EQ - Karadere 496 NS	10.11	0.46	0.08	0.05	0.07	0.06
Duzce EQ - Karadere 498 EW	3.47	0.26	0.04	0.07	0.04	0.05
Duzce EQ - Karadere 498 NS	3.90	0.35	0.04	0.07	0.05	0.06

The east-west component of the DZC record of the November 1999 earthquake (PGA = 0.51g) created the highest displacement demand on the members (Fig. 11). The other records of the same earthquake such as BOL (PGA = 0.8g), 496 (PGA = 1.0g) and 375 (PGA = 0.8g) did not force the structure over the limits foreseen in its design which is 0.32 m. The observed relative movement of the girders in the longitudinal direction exceeded 1 m at some piers. However, the maximum calculated response in the analyses stayed within the 0.5-m displacement capacity of the EDU.

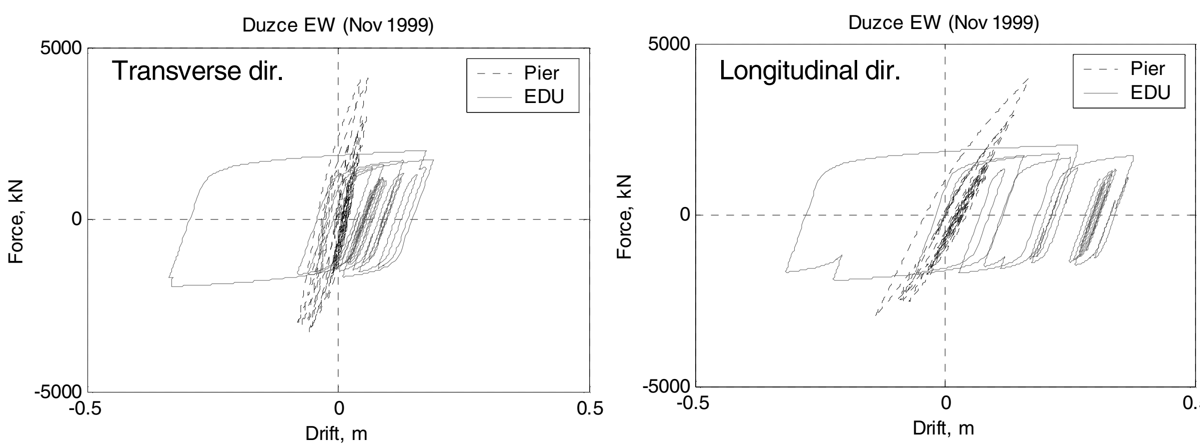

Figure 11. The hysteresis curves of the elements in the analysis with record DZC-EW (Nov.)

The results of the analyses showed that the maximum EDU response is not proportional to the PGA of the input ground motion. The graphical presentation of the maximum EDU drifts and the peak ground accelerations in Fig. 12 reveals the scatter in the results more clearly. A better correlation was observed between the maximum response of EDU and the PGV of the selected ground motions.

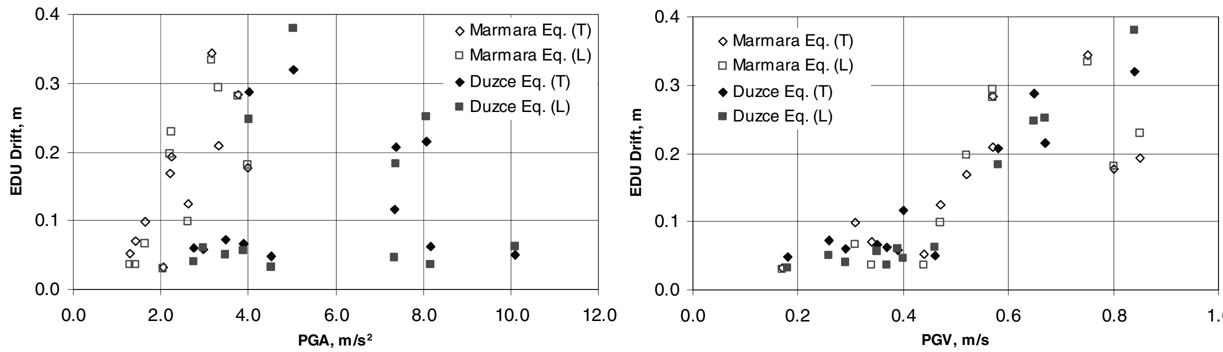

Figure 12. The correlation of the maximum EDU drift with the PGA and PGV of the records

INELASTIC RESPONSE OF THE VIADUCT TO THE GROUND DEFORMATION

The Model

The response of the viaduct was evaluated by analyzing its 2-dimensional model including all the piers and the deck segments with computer software Drain-2Dx [9, 10].

The piers were represented by elastic frame elements with two plastic springs at the ends. The mass of each pier element was distributed to the nodes along the height. The plastic hinge properties were based on the moment-curvature of the base section of the piers. The pier caps were represented by two rigid-frame elements placed on top of each pier horizontally as shown in Fig. 13. Its mass was distributed to the far ends.

The truss elements connecting the pier cap and the deck were used to simulate the nonlinear characteristics of the EDU's. The diagonal truss elements contributed to the lateral resistance of the deck both in tension and compression whereas the rigid vertical members were placed only for stability. The elasticity modulus and the cross-sectional area were selected in such a way that the axial stiffness of each diagonal member became equal to the initial stiffness of the EDU's.

In the observed state of the structure after the earthquake, the amount of relative movement between girders and pier cap was high enough not only to close the 0.5-m gap between center girders and plinths but also to break the plinths. The initial gap between the girders and the plinth is approximately equal to the displacement capacity of the EDU's. Therefore, the EDU's must have failed at the instant of contact between plinths and girders. The effect of the shear failure of the plinths on the response was included in the model by introducing the diagonal gap elements placed as shown in Fig. 13. The lateral stiffness of the plinths was calculated to be 14E6 kN/m by combining its flexural, shear and slip characteristics as proposed by Sozen and Moehle [11]. The calculation of the shear strength of the plinths was based on the shear-friction formula in ACI 318-02 [12].

Each deck segment was represented by linear-elastic frame elements between the piers. There were two different types of members for the deck: (1) the composite section including the girders and the top slab, (2) the short length of spans between them. These members were assumed to be axially rigid. There was no indication of axial deformation of these members observed after the earthquake. The tributary mass of the deck for each pier, 1540 kN, was lumped at the nodes at the deck level.

Between the deck segments were the gap elements that allow 0.64 m shortening of the elements before acting in compression. These members did not transfer shear or moment. The stiffness, after the closing of the gap, was set to a very high value making it practically incompressible. The gap elements used at the abutments allowed a closing of only 0.25 m.

The mathematical model of the complete structure included a damping factor of 2%. Drain-2DX uses mass proportional damping.

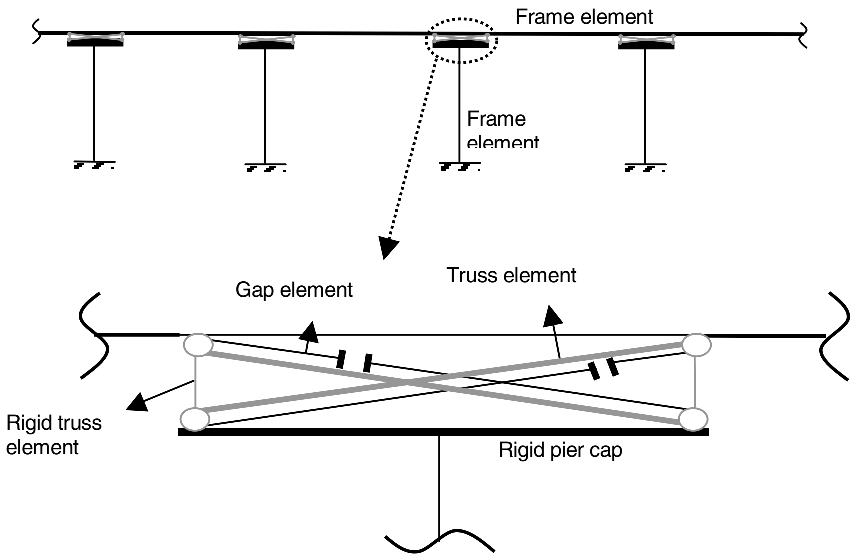

Figure 13. The elements of the model of the viaduct for ground deformation analyses

Dynamic Pier Movements

The ground deformation at the viaduct site caused the permanent displacement of the piers. The main component of the movement is along the axis of the viaduct. The absolute displacement of each individual pier was estimated from the measurements of the structure and the observations of the plate movements (Fig. 7). In the analysis, the piers were moved from their initial positions to the final positions within a few seconds. The pier displacement function was defined by Eq.13 which describes movement of a particle from position 0 to D_{max} in duration T_p.

$$D = D_{max}\left(\frac{t}{T_p} - \frac{1}{2\pi}\sin\frac{2\pi t}{T_p}\right) \qquad (1)$$

The velocity function corresponding to the given displacement function is as follows:

$$V = V_{max}\left(\frac{1}{2} - \frac{1}{2}\cos\frac{2\pi t}{T_p}\right) \qquad (2)$$

By equating the integral of Eq.2 to D_{max}, T_p can be expressed as $2D_{max}/V_{max}$.

In all the analyses, the maximum ground movement was set at 1.4 m at the west abutment and 0.7 m at the east abutment (Fig.14). The maximum ground velocity at the site is not a measured quantity or cannot be inferred from any other evidence at or near the site of the viaduct. Therefore, it was changed within a range of 0.75 m/s to 3 m/s to investigate its effect on the structural response. The amplitude of the movement was scaled for each pier on the same side of the fault. The duration of the movement for each pier was equal to the duration of the movement of the abutment moving in the same direction with that pier. There was no phase lag between the movements of the piers or the abutments in the analyses.

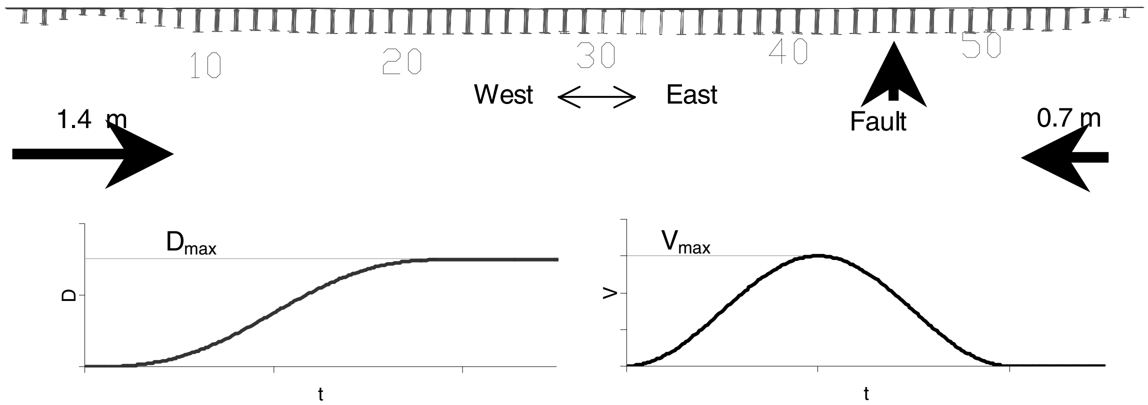

Figure 14. Movement at the abutments

Response of the Viaduct to Short-Duration Pier Movement

In the undeformed state of the structure, the girders were supported on bearing pads which permitted the girders move on the piers hampered by a minimum of friction. A sudden displacement of the pier bases in one direction causes the relative movement of the girders in the reverse direction with respect to the piers. This phenomenon is similar to what passengers experience in an accelerating vehicle. If the motion stops before failure of the EDU's and the bearings, the force stored in the EDU's can re-position the girders. However, if the relative movement is large enough to cause the girders to fall off the low-friction bearings, the girder will remain essentially at its maximum excursion.

Figure 15 illustrates the response of the viaduct to the proposed type of ground movement as a whole. Each "girder" in the figure represents one 10-span segment of the viaduct. The clear distance between the girders is 0.65 m. The clear distance at the abutments are 0.25 m initially. All the members seen in the figure are rigid. The ground is represented by three rigid blocks. The movements of the blocks are shown in the figure. Block A moves 1.4 m east, Block B moves 0.7 m east and Block C moves 0.7 m west. The relative movement of the blocks reduces the distance between the piers of Segment 4 and 5. The maximum velocities of the abutments are assumed to be equal. The movement of the west abutment takes longer than the movement of the east abutment because the magnitudes of their absolute movements are different.

The response of the viaduct to the ground deformation illustrated can be thought of as a series of events as shown in Fig. 15:

- Between t_0-t_1: Segments 1-4 shift west and Segment 6 shifts east relative to the piers. The direction of the relative movement is the same for both ends of each of these segments. Because the piers of Segment 5 move toward each other, the relative movements at the two ends of Segment 5 are in the opposite directions.
- Time t_1: The east abutment impacts Segment 6 and the direction of the relative movement of Segment 6 is reversed. The other segments continue their relative movements.
- Time t_2: The west abutment impacts Segment 1 and reverses its direction of relative movement.
- Between t_2-t_3: After the two end segments (Segments 1 and 6) bounce off the abutments, they move toward the adjacent segments (Segments 2 and 5). Segment 6 reaches its original position relative to its supports and then moves farther west. Segments 2 and 3 continue to move west (relative movement). The two ends of Segment 5 continue to move in opposite directions with respect to the piers underneath.
- Time t_3: Segments 5 and 6 collide with each other and bounce back.
- Time t_4: Segments 1 and 2 collide with each other. At the time of collision, Segment 2 is at the edge of its supports. Segment 5 impacts Segment 4 and bounces back.

- Between t_4-t_5: Segments 2, 3 and 4 fall off their supports and remain at their maximum excursions. Segment 1 is trapped between the west abutment and Segment 2. The relative movement of the west end of Segment 5 also exceeds the seating length on the support and Segment 5 falls off the support.
- Time t_5: Segment 5 impacts Segment 6.

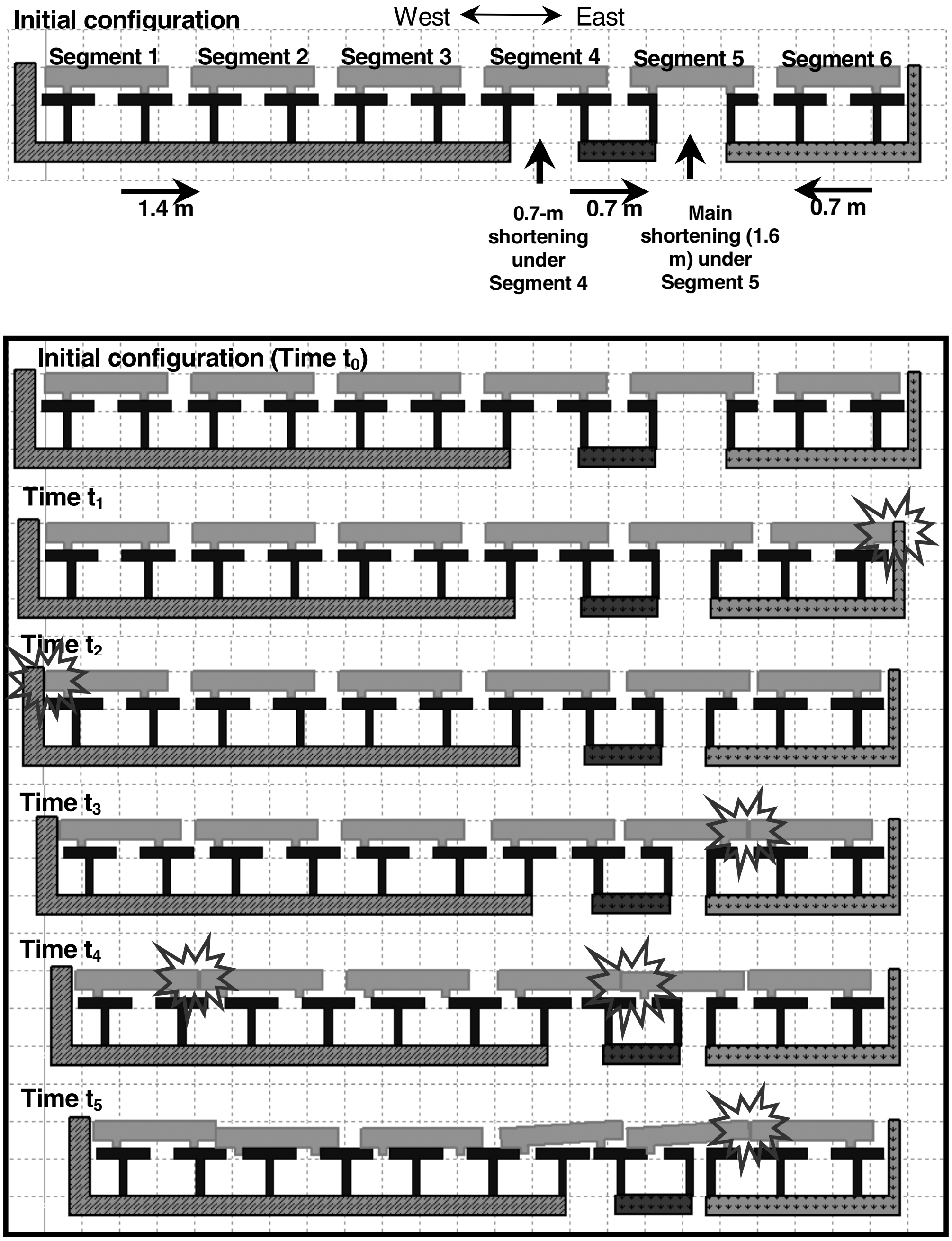

Figure 15. Illustration of the dynamic response of the viaduct to the ground deformation. Each girder shown in the figure corresponds to one 10-span segment of the structure.

The relative positions of the six segments at time t_5 correspond to the observed positions of the viaduct segments after the earthquake suggesting that the series of the events described above provides an explanation of how the viaduct responded to the ground distortion. The observed damage of the structural components of the viaduct confirms the events in the series. This phenomenon will be analyzed quantitatively in the next section.

Effect of the Maximum Ground Velocity on the Response of the Viaduct

The nonlinear response to ground deformation calculated using Drain-2Dx is presented in the form of the final relative locations of the girders with respect to the ground. The response calculations were performed for three values of V_{max}: 1.0, 1.5 and 2.0 m/s. The pier movements are completed in 2.8, 1.9 and 1.4 s, respectively. The analyses were performed for the response of the right and the left carriageways.

The calculated responses are presented in Fig. 16 in comparison with the measurements of the deformed state of the carriageways. The graphs present the relative movement of the deck segments with respect to the pier bases (or the ground). The westward relative movements of the piers are indicated by the positive values in the figures. The relative-movement pattern of the structure observed after the earthquake is, in general, good agreement with the results of the analysis. The maximum ground velocity selected for the ground motion in each solution changes the amplitude of the relative displacement of the segments.

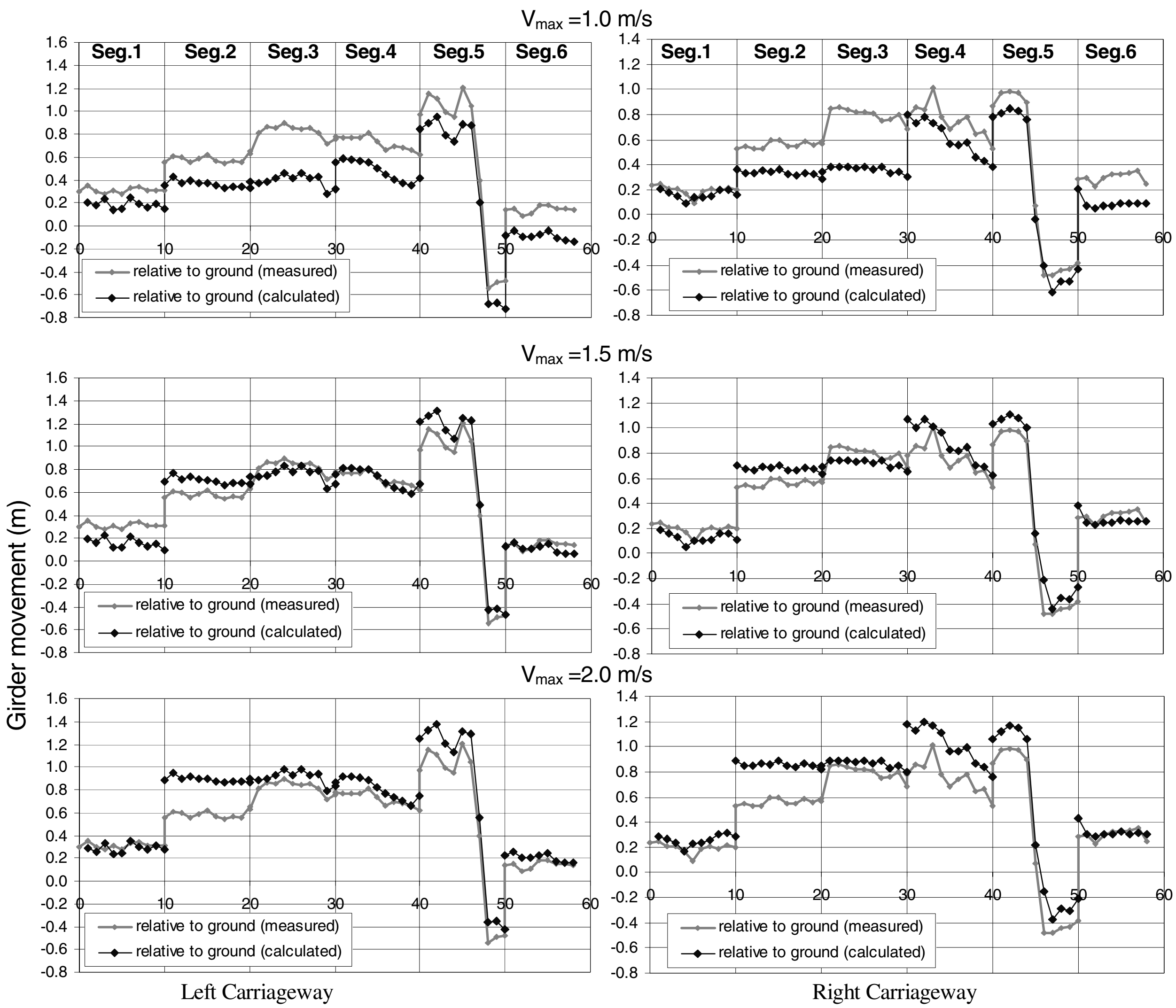

Fig. 16. Comparison of the results of analyses with the measurements of the deformed state of the structure.

The best match in the analyses is obtained for the maximum ground velocity of 1.5 m/s. In the analysis for V_{max}= 1.0 m/s, the maximum relative movement of Segments 2 and 3 is less than the 0.5-m initial clear distance between the girders and the plinth. Furthermore, Segment 6 does not develop sufficient westward movement to match the observed relative movement. In analyses for V_{max}= 1.5 m/s and V_{max}= 2.0 m/s, the calculated response is quantitatively similar to the observed state of the viaduct. The most significant difference between the two analyses is observed in Segments 2 and 4. In the analysis for V_{max}= 2.0 m/s, the relative displacement of these segments is overestimated by 0.25 m.

CONCLUSIONS

The field observations after the 1999 Turkey and Taiwan earthquakes showed that if a structure is crossed by surface rupture of an earthquake, changes in its foundation layout imposed by the deformation of the ground are likely to be permanent. Depending on the type of the rupture and its orientation relative to structure, these changes might be in the form of elongation or shortening of the spans, or differential vertical movement of the supports. The supports also might tilt, twist or rotate while displacing. Especially for long surface structures built in active fault regions, the possibility of such effects might be very high; therefore they should be designed to sustain differential permanent movement of the supports. It is also important to note the obvious: devices for energy dissipation will not function if there is a significant span length change or relative vertical movement.

The Bolu Viaduct was damaged by the 17 August 1999 Marmara and 12 November 1999 Duzce, Turkey earthquakes. The surface rupture of the Duzce earthquake crossed the viaduct changing the pier layout permanently. The relative movement of the girders with respect to the piers caused the failure of the energy dissipating units (EDU) and their plinths.

The nonlinear response of the Bolu Viaduct was evaluated for all high-demand ground motion records obtained in the vicinity of the viaduct during the August and November 1999 earthquakes in Turkey (Table 1). None of these analyses resulted in relative motion between the girders and the piers large enough to saturate the displacement limits of the EDU.

The response of the Bolu Viaduct was analyzed using as base input the relative motions of the pier bases to simulate the surface slip, assuming that these motions occurred at the beginning of the earthquake. The measured shortening of the viaduct was 2.1 m. Three solutions were obtained assuming that the observed shortening occurred at velocities of 1.0, 1.5 and 2.0 m/s. All three solutions led to permanent relative displacements of the girders that compared favorably with the observations. Best results were obtained at 1.5 m/s. The results suggest that the severe damage to the viaduct was caused by the rapid distortion of the ground.

The analyses indicate that EDU response is better correlated with peak ground velocity (PGV) than with peak ground acceleration (PGA).

Acknowledgments

This research was sponsored by the National Science Foundation (Grant No. 85270-CMS). Opinions, findings, conclusions, and recommendations included in the paper are those of the authors listed and do not reflect the views of the National Science Foundation. The writers are grateful to ASTALDI-BAYINDIR Co., and Prof. Cetin Yilmaz of the Middle East Technical University for making the survey data of the viaduct available.

References

1. EERI. 2001."Chi-Chi, Taiwan, Earthquake of September 21, 1999 Reconnaissance Report", *Earthquake Spectra*, Supplement A to Volume 17, Earthquake Engineering Research Institute, Publication 2001-02.
2. NCREE, 2000. *Investigation Report on Bridge Damage in Chi-Chi Earthquake on September 21,1999,* National Center for Research on Earthquake Engineering, Taiwan.
3. METU. 2000. *Engineering Report on the Marmara and Duzce Earthquakes*, Middle East Technical University, Civil Engineering Department, Turkey. (Turkish)
4. Marioni A. 2000. *Behavior of Large Base Isolated Prestressed Concrete Bridges During the Recent Exceptional Earthquakes in Turkey*, http://192.107.65.2/GLIS/ HTML/gn/turchi/g5turchi.htm (online).
5. Akyuz, H.S., Hartleb, R., Barka, A., Altunel, E., Sunal, G., Meyer, B. and R. Armijo. 2002. "Surface rupture and slip distribution of the 12 November 1999 Duzce Earthquake (M 7.1), North Anatolian Fault, Bolu, Turkey," *Bulletin of Seismological Society of America*, 92, No.1, pp.61-66.
6. Burgmann, R. 2002. *Data and Models of 1999 Izmit and Düzce Earthquakes*, Active Tectonics Research Group, University of California at Berkeley, http://www.seismo.berkeley.edu/~burgmann /RESEARCH/ TURKEY/turkey.html. (online)
7. Gur T. and M.A. Sozen. 2004. "An Investigation of the Effects of the 1999 Anatolian Earthquakes on the Bolu Viaduct", Procedings of the 4th National Seismic Conference on Bridges and Highways, February 9-11, 2004, Memphis, TN.
8. Ramberg W. and W. R. Osgood. 1943. *Description of Stress-Strain Curves by Three Parameters*, National Advisory Committee of Aeronautics, Technical Note 902.
9. Prakash V., Powell G.H. and S. Campbell. 1993. *Drain-2Dx Base Program Description and User Guide, Version 1.10*, University of California at Berkeley, Report No. UCB/SEMM 93-18, Berkeley, CA.
10. Powell G.H. 1993. *Drain-2Dx Element Description and User Guide for Element Type01, Type02, Type04, Type06, Type09, and Type15*, University of California at Berkeley, Report No. UCB/SEMM 93-18, Berkeley, CA.
11. Sozen M.A. and J.P. Moehle. 1993. *Stiffness of Reinforced Concrete Walls Resisting In-Plane Shear*, prepared for Electric Power Research Institute, Research Project 3094-01, Palo Alto, CA.
12. ACI Committee 318. 2002. *Building Code Requirements for Structural Concrete (ACI 318-02) and Commentary (ACI 318R-02)*, American Concrete Institute, Farmington Hills, Mich. p.89.